

Electronic Supplementary Information

Ultralow-Intensity Near-Infrared Light Induces Drug Delivery by Upconverting Nanoparticles

Shuqing He,^a Kristina Krippes,^a Sandra Ritz,^a Zhijun Chen,^a Andreas Best,^a Hans-Jürgen Butt,^a
Volker Mailänder^{ab} and Si Wu*^a

^a Max Planck Institute for Polymer Research, Ackermannweg 10, 55128 Mainz, Germany.

E-mail: wusi@mpip-mainz.mpg.de

^b III. Medical Clinic, University Medicine of the Johannes-Gutenberg University Mainz,
Langenbeckstr. 1, 55131 Mainz, Germany.

Materials

Ytterbium(III) acetate hydrate (99.9%) and (3-Aminopropyl) triethoxysilane (98%) were purchased from Alfa Aesar. ω -trimethoxysilane terminated poly(ethylene glycol) methyl ether (PEG, $M_n = 0.35$ kg/mol and $PDI = 1.10$) was purchased from Polymer Source. Slide-A-Lyzer MINI dialysis devices (10K MWCO) was purchased from Thermo Fisher Scientific. The spiropyran derivative (SP) 1-(2-hydroxyethyl)-3,3-dimethylindolino-6'-nitrobenzopyrylospiran (93%) and the diarylethene derivative (DTE) 1,2-bis(2,4-dimethyl-5-phenyl-3-thienyl)-3,3,4,4,5,5-hexafluoro-1-cyclopentene (98%) were purchased from TCI Europe. Thulium(III) acetate hydrate (99.9%), Yttrium(III) acetate hydrate (99.9%), 2,2'-bipyridine (98%), folic acid (bioreagent, $\geq 97\%$), Dowex® 22 Cl anion-exchange resin, trimethylphosphine solution (1.0 M in THF), Lithium chloride ($\geq 99\%$), 1-Octadecene (technical grade, 90%), oleic acid (technical grade, 90%), ammonium fluoride ($\geq 99.99\%$), ruthenium(III) chloride trihydrate (technical), potassium hexafluorophosphate (98%), hexadecyltrimethylammonium bromide ($\geq 98\%$), tetraethyl orthosilicate (98%), doxorubicin hydrochloride (98%), fluorescein 5(6)-isothiocyanate ($\geq 90\%$), N-hydroxysuccinimide (NHS, 98%), N-ethyl-N'-(3-dimethylaminopropyl)carbodiimide hydrochloride (EDC, $\geq 99\%$), azobenzene (98%), phosphate buffered saline (BioPerformance Certified, pH 7.4), and MCM-41 type mesoporous silica nanoparticles were purchased from Sigma-Aldrich. All other solvents were purchased from Sigma-Aldrich or Fisher Scientific. The o-nitrobenzyl derivative (NB) 4,5-dimethoxy-2-nitrobenzyl (3-(triethoxysilyl)propyl)carbamate was synthesized according to a literature method.^[1]

Characterization

UV/Vis/NIR absorption spectra were measured on a Lambda 900 spectrometer (Perkin Elmer). Transmission electron microscopy (TEM) images were measured on a JEOL JEM1400 Transmission Electron Microscope. Fluorescence spectra were recorded on a TIDAS II spectrometer (J&M). X-ray diffraction (XRD) patterns were measured on a Fine focus anode system with Cu K α line ($\lambda = 0.15418$ nm). Dynamic light scattering (DLS) measurements were performed on a commercially available instrument from ALV GmbH consisting of a goniometer and an ALV-5000 multiple-tau full-digital correlator. The DLS measurements were performed at the scattering angle of 90° with a 532 nm laser. Nitrogen adsorption-desorption isotherms were obtained at 77 K on a TriStar 3020 accelerated surface area and pore size analyzer. FTIR spectra

were recorded using a Nicolet 730 FTIR spectrometer. ^{29}Si MAS solid-state nuclear magnetic resonance (NMR) spectra were recorded on a Bruker 300 MHz spectrometer. Upconversion photoluminescence measurements were performed on a Spex Fluorolog II (212) spectrometer. A diode laser at 974 nm (type P976MF, Photon tec Berlin GmbH) coupled with a 105 μm (core) fiber was employed as the excitation source. The diode laser can be equipped with an adjustable fiber collimator (Changchun New Industries Optoelectronics Technology). The output power of the diode laser was controlled by a tabletop laser driver (device type ds11-la12v08-pa08v16-t9519-254-282, OsTech GmbH i.G. electro-optical-instruments). The output power density of the diode laser was measured by an optical power meter (Model 407A, Spectra-Physics Corporation) and a NIR indicator (Newport, Model F-IRC1).

Synthesis

Synthesis of $\beta\text{-NaYF}_4$: 0.5 mol% Tm^{3+} , 30 mol% Yb^{3+} core nanoparticles. The $\text{NaYF}_4\text{:TmYb}$ core nanoparticles were synthesized according to a literature method.^[2] $\text{Y}(\text{CH}_3\text{COO})_3 \cdot x\text{H}_2\text{O}$ (372 mg, 1.4 mmol), $\text{Yb}(\text{CH}_3\text{COO})_3 \cdot x\text{H}_2\text{O}$ (210 mg, 0.6 mmol) and $\text{Tm}(\text{CH}_3\text{COO})_3 \cdot x\text{H}_2\text{O}$ (3.5 mg, 0.01 mmol) were added to a 100 mL threeneck round-bottom flask containing octadecene (30 mL) and oleic acid (12 mL). The solution was stirred magnetically and heated to 120 $^\circ\text{C}$ under vacuum (heating rate: 3 $^\circ\text{C}/\text{min}$) to form the lanthanide oleate complexes. The solution was degased at 120 $^\circ\text{C}$ for 15 min to remove residual water, acetic acid and oxygen. The temperature of the solution was then lowered to 50 $^\circ\text{C}$ and the reaction flask was placed under a gentle flow of Ar. During this time, a solution of ammonium fluoride (296 mg, 8.0 mmol) and sodium hydroxide (200 mg, 5.0 mmol) dissolved in methanol (20 mL) was prepared via sonication. Once the reaction mixture reached 50 $^\circ\text{C}$, the methanol solution was added to the reaction flask and the resulting cloudy mixture was stirred for 30 min at 50 $^\circ\text{C}$. The reaction temperature was then increased to ~ 70 $^\circ\text{C}$ and degased for 15 min to remove methanol in the reaction flask. Then, the reaction flask was placed under a gentle flow of Ar. Subsequently, the reaction temperature was increased to 300 $^\circ\text{C}$ (heating rate: 20 $^\circ\text{C}/\text{min}$) under the Ar flow and kept at this temperature of 90 min. During this time the reaction mixture became progressively clearer until a completely clear, slightly yellowish solution was obtained. The mixture was allowed to cool to room temperature naturally. The nanoparticles were precipitated by the addition of ethanol (~ 80 mL)

and isolated via centrifugation at 5000 rpm. The resulting pellet was dispersed in a minimal amount of hexane (5-10 mL) and precipitated with excess ethanol (~60 mL). The nanoparticles were isolated via centrifugation at 5000 rpm and then dispersed in hexane (10–15 mL) for the subsequent shell growth procedure. The synthesized nanoparticles are characterized by TEM (Figure S2), DLS (Figure S3), and XRD (Figure S4).

Synthesis of β -NaYF₄: 0.5 mol% Tm³⁺, 30 mol% Yb³⁺ / β -NaYF₄ core/shell nanoparticles.

The NaYF₄:TmYb@NaYF₄ upconverting nanoparticles (UCNPs) were synthesized according to a literature method.^[2] Y(CH₃COO)₃•xH₂O (479 mg, 1.8 mmol) was added to a 100 mL threeneck round-bottom flask containing octadecene (30 mL) and oleic acid (12 mL). The solution was stirred magnetically and heated to 120 °C under vacuum (heating rate: 3 °C/min) and maintain at 120 °C for 15 min. The temperature of the reaction flask was lowered to 80 °C and the reaction flask was placed under a gentle flow of Ar. Then, the dispersion of NaYF₄: 0.5 mol% Tm³⁺, 30 mol% Yb³⁺ core nanoparticles in hexane, which was synthesized by the procedure shown above, was added to the flask. The resulting solution was heated to 110 °C (heating rate: 5 °C/min) and degassed for 15 min to remove hexane in the reaction flask. The reaction mixture was cooled to 50 °C and the flask was place under a gentle flow of Ar. Then, a solution of ammonium fluoride (259 mg, 7.0 mmol) and sodium hydroxide (175 mg, 4.4 mmol) in methanol (20 mL) was added. The resulting cloudy mixture was stirred at 50 °C for 30 min. The reaction temperature was then increased to ~70 °C and degassed for 15 min to remove methanol in the reaction flask. Then, the reaction flask was placed under a gentle flow of Ar. Subsequently, the reaction temperature was increased to 300 °C (heating rate: 20 °C/min) and kept at this temperature for 90 min under the Ar flow. The mixture was allowed to cool to room temperature naturally. The nanoparticles were precipitated by the addition of ethanol (~80 mL) and isolated via centrifugation at 5000 rpm. The resulting pellet was dispersed in a minimal amount of hexane (5-10 mL) and precipitated with excess ethanol (~60 mL). The nanoparticles were isolated via centrifugation at 5000 rpm and then stored in cyclohexane (15 mL). The synthesized nanoparticles are characterized by TEM (Figure S2), DLS (Figure S3), XRD (Figure S4) and UV/Vis absorption spectroscopy (Figure S5).

Synthesis of UCNP@mSiO₂ nanoparticles. UCNPs with mesoporous silica shell were synthesized using a modification of recently reported procedures.^[3] In general, the mesoporous silica layer was prepared by the sol-gel reaction of tetraethyl orthosilicate (TEOS) in an aqueous solution containing cetyltrimethylammonium bromide (CTAB). First, NaYF₄:TmYb@NaYF₄ UCNPs in cyclohexane (0.1 M, 0.5 mL) were added in an aqueous solution CTAB (5 mL, 0.05 M). The resulting solution was stirred for 1 h to form an oil-in-water emulsion. The mixture was heated up to 80 °C and maintained at the temperature for 30 min to evaporate cyclohexane. The resulting solution was added in a mixture of water (25 mL) and an aqueous solution of NaOH (1.8 mL, 2 M). The mixture was heated to 70 °C under stirring. Then, TEOS (0.3 mL) and ethyl acetate (1.8 mL) were added to the reaction mixture. The reaction was maintained at 70 °C for 12 hours. The nanoparticles were isolated via centrifugation at 5000 rpm and washed with ethanol and stored in ethanol (20 mL). To extract CTAB from the nanoparticles, HCl (40 µL) was added to the dispersion to adjust pH of the solution to ~1.4). The dispersion was stirred for 3 h at 60 °C. The nanoparticles were isolated via centrifugation at 5000 rpm and washed with ethanol. The UCNP@mSiO₂ nanoparticles were stored in ethanol. The synthesized nanoparticles are characterized by TEM (Figure S2), DLS (Figure S3), and surface area and pore size analyzer (Figure S7).

Synthesis of the ruthenium complex Ru[(2,2'-bipyridine)₂(trimethylphosphine)((3-Aminopropyl) triethoxysilane)](PF₆)₂ (Ru1). Ru1 was synthesized according to a literature method.^[4]

Synthesis of UCNP@mSiO₂-Ru nanoparticles by capping UCNP@mSiO₂ nanoparticles with Ru1. Aqueous solution of NaOH (10 µL, 1 M) were added to the suspension of UCNP@mSiO₂ nanoparticles (~25 mg) and Ru 1 (2.3 mg) in ethanol (25 mL). The mixture was stirred for 12 hours at room temperature. UCNP@mSiO₂-Ru nanoparticles were collected by centrifugation at 7000 rpm and washed by ethanol. The synthesized nanoparticles are characterized by ²⁹Si MAS solid-state NMR (Figure S8), UV/Vis absorption spectroscopy (Figure S9), and FTIR (Figure S10). The amount of Ru complexes grafted on the nanoparticles calculated by UV/Vis absorption spectroscopy is ~7.6 µg Ru complexes on 1 mg nanoparticles (Figure S11).

Preparing DOX-UCNP@mSiO₂ nanoparticles by loading UCNP@mSiO₂ nanoparticles with doxorubicin. Doxorubicin hydrochloride (1 mg) was dissolved in ethanol (25 mL). UCNP@mSiO₂ nanoparticles (~25 mg) were added in the ethanol solution of doxorubicin. The mixture was kept in the dark and stirred at room temperature for 24 hours. Then, the UCNP@mSiO₂ nanoparticles loaded doxorubicin (DOX-UCNP@mSiO₂) was separated by centrifugation at 7000 rpm. The drug loading efficiency measured by fluorescence spectroscopy and UV/Vis absorption spectroscopy is 2.36% and 2.52% (23.6 and 25.2 µg doxorubicin in 1 mg nanoparticles), respectively (Figure S17).

Synthesis of DOX-UCNP@mSiO₂-Ru nanoparticles by capping DOX-UCNP@mSiO₂ nanoparticles with Ru1. Synthesis of DOX-UCNP@mSiO₂-Ru nanoparticles was using the same procedure as that of UCNP@mSiO₂-Ru nanoparticles, except for changing UCNP@mSiO₂ to DOX-UCNP@mSiO₂ as the starting material.

Synthesis of fluorescence-labeled UCNP@mSiO₂-Ru nanoparticles (UCNP@mSiO₂-Ru-FITC). The fluorescence-labeled nanoparticles were synthesized by using a modification of a literature method.^[5] UCNP@mSiO₂-Ru nanoparticles (~10 mg) dispersed in ethanol (20 mL) were modified by (3-Aminopropyl) triethoxysilane (100 µL) at room temperature. A fluorescent dye fluorescein 5(6)-isothiocyanate (FITC, 1 mg) was added to the ethanol dispersion. The mixture was stirred for 24 h at room temperature. Nanoparticles were obtained by centrifugation at 5000 rpm and washing with ethanol and water. Finally, the nanoparticles were store in water.

Synthesis of poly(ethylene glycol) (PEG) and folic acid (FA) modified DOX-UCNP@mSiO₂-Ru nanoparticles. PEG- and FA-modified nanoparticles were prepared by using a modification of recently reported procedures.^[5-6] ω-trimethoxysilane terminated PEG (15 µL) was added to a mixture of ethanol (15 mL), deionized water (3 mL), ammonia (150 µL, 28%), and DOX-UCNP@mSiO₂-Ru nanoparticles (~10 mg). After stirred for 24 hours, nanoparticles were obtained by centrifugation at 7000 rpm. The obtained nanoparticles were washed with dimethyl sulfoxide (DMSO). Then, PEG-modified DOX-UCNP@mSiO₂-Ru nanoparticles were dispersed in DMSO. FA (0.5 mg) and (3-Aminopropyl) triethoxysilane (2.5 µL) were dissolved in DMSO

(1.5 mL). Subsequently, NHS (0.55 mg) and EDC (0.8 mg) were added into the mixture and stirred for 2 hours. PEG-modified DOX-UCNP@mSiO₂-Ru nanoparticles (~10 mg) in DMSO (1.5 mL) were added to the reaction mixture. The reaction mixture was stirred at room temperature overnight. PEG- and FA-modified DOX-UCNP@mSiO₂-Ru nanoparticles were obtained by centrifugation at 7000 rpm. The nanoparticles were washed by DMSO and ethanol and dried under vacuum at 50 °C for 24 hours. The nanoparticles were dispersed in water before use. The nanoparticles are characterized by TEM (Figure S15). UV/Vis absorption spectroscopy shows that ~1.25 µg FA was grafted on 1 mg nanoparticles (Figure S16).

Synthesis of PEG- and FA-modified UCNP@mSiO₂-Ru. Synthesis of PEG- and FA-modified UCNP@mSiO₂-Ru nanoparticles was using the same procedure as that for PEG- and FA-modified DOX-UCNP@mSiO₂-Ru nanoparticles, except for changing DOX-UCNP@mSiO₂-Ru to UCNP@mSiO₂-Ru as the starting material. The nanoparticles are characterized by TEM (Figure S15).

Synthesis of PEG- and FA-modified UCNP@mSiO₂-Ru-FITC. Synthesis of PEG- and FA-modified UCNP@mSiO₂-Ru-FITC nanoparticles was using the same procedure as that for PEG- and FA-modified DOX-UCNP@mSiO₂-Ru nanoparticles, except for changing DOX-UCNP@mSiO₂-Ru to UCNP@mSiO₂-Ru-FITC as the starting material.

Synthesis of PEG- and FA- modified DOX-mSiO₂-Ru nanoparticles. Synthesis of PEG- and FA-modified DOX-mSiO₂-Ru nanoparticles was using the same procedure as that for PEG- and FA-modified DOX-UCNP@mSiO₂-Ru nanoparticles, except for changing UCNP@mSiO₂ to commercial MCM-41 type mesoporous silica nanoparticles (Sigma Aldrich, CAS No. 7631-86-9, pore size 2.1-2.7 nm) as the starting material.

Near-infrared light-triggered drug release

Release profile of doxorubicin was measured by the dialysis method (Figure S19).^[7] PEG and FA-modified DOX-UCNP@mSiO₂-Ru nanoparticles in PBS buffer were placed in a dialysis device (Slide-A-Lyzer MINI Dialysis Device, 10K MWCO, Thermo Fisher Scientific) on top of a cuvette. The nanoparticles were irradiated by a NIR laser at 974 nm for different time at

different power densities. After every exposure (30 min or 1 hour), we wait for 1 hour to let the released doxorubicin to diffuse into the cuvette. The amount of released doxorubicin is determined by fluorescence spectroscopy (Figure S19).

Cell culture

HeLa cells were obtained from DSMZ (Deutsche Sammlung für Mikroorganismen und Zellen, Germany) and were cultured and kept in Dulbecco's Modified Eagle's Medium (DMEM, Sigma-Aldrich, USA) supplemented with 10 % fetal bovine serum (FBS, Invitrogen, USA) and 1 % penicillin/streptomycin (Life technologies, USA) in an incubator at 37 °C, 95 % humidity and 5% CO₂ (Labotec, Germany). Treatment with trypsin (0.05 %) (Life technologies, USA) for 5 minutes was employed to detach the cells for further assays.

Cell imaging by confocal laser scanning microscopy (cLSM)

For cLSM studies, 4×10^4 HeLa cells per milliliter were seeded in 35 mm diameter coverslip dishes (IBIDI, Germany) and cultured for 24 h in complete DMEM (Phenol red free for cLSM). Cell medium was then replaced by fresh DMEM containing 300 µg/mL FITC-labeled nanoparticles. The cells were incubated for another 24 h before residual nanoparticles were removed by washing two times with Dulbecco's phosphate buffered saline (DPBS) (Sigma-Aldrich, Germany). Live cell images were taken with a commercial setup (LSM SP5 STED Leica Laser Scanning Confocal Microscope, Leica, Germany), consisting of an inverse fluorescence microscope DMI 6000 CS equipped with a multi-laser combination, five detectors operating in the range of 400-800 nm. A HCX PL APO CS 63 x 1.4 oil objective was used for these studies and were excited and detected in a sequential mode under the following conditions: Fluorescent nanoparticles were excited with a laser (514 nm, ~0.8 mW), detected at 533-570 nm and pseudocolored in green; The cell membrane was stained with CellMaskOrange (2.5 mg/mL, Invitrogen, Germany), excited with a DPSS laser (561 nm, ~1.3 mW), detected at 570-640 nm, pseudocolored in red; The cell nucleus was stained with DraQ5 (2.5×10^{-6} M, Biostatus, UK), excited with a HeNe laser (633 nm, ~0.4 mW), detected at 650-760 nm and pseudocolored in blue. The cLSM images are shown in Figure 4a and Figure S21.

Cell viability

All mentioned *in vitro* cytotoxicity/phototoxicity measurements were assessed by CellTiter-Glo Luminescent Cell Viability Assay (Promega, USA), which determines the number of viable cells based on ATP quantitation as an indicator for metabolically active cells. CellTiter-Glo assay was performed according to the manufacturer's protocol. Luminescence was monitored using a Platereader Infinite M1000 (Tecan, Germany). Cytotoxicity/phototoxicity was expressed as the percentage of cell viability compared to untreated control cells. HeLa cells were seeded in 96-well plates (Greiner Bio One, Germany) at a density of 7.5×10^4 cells per well and cultured for 24 h. To determine the cytotoxicity of various nanoparticles without NIR irradiation, they were added to the culture medium and cell viability was assessed after 24 hours of incubation. To investigate the impact of NIR irradiation alone, cells were irradiated by the NIR laser at 974 nm (L4-9897510-100M, JDS Uniphase Corporation) and cell viability was assessed after 24 hours. To examine the drug release from nanoparticles, 300 $\mu\text{g}/\text{mL}$ were added to the culture medium for 3-6 hours followed by exposure to different NIR dosage. Cell viability was assessed after a terminal incubation time of 24 hours. Viability of HeLa cells is shown in Figure S22.

974 nm NIR light irradiation on cells

For laser irradiation experiments, HeLa cells were seeded in 96-well plates at a density of 7.5×10^4 cells per well and cultured for 24 hours. Irradiation took either place after 3-6 hours of incubation with nanoparticles, or without adding any nanoparticles. The experiments were performed at room temperature. A continuous wave NIR laser (974 nm, $0.35 \text{ W}/\text{cm}^2$, device type L4-9897510-100M, JDS Uniphase Corporation) was used to irradiate cells. The irradiation time varied from 0–30 minutes. Viability of HeLa cells after 974 nm light irradiation is shown in Figure 4b, 4c, S23, S24.

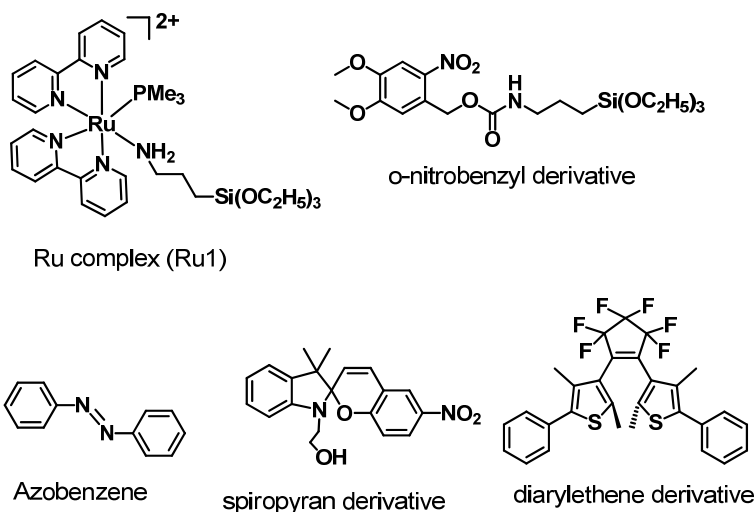


Figure S1. Chemical structures of five photosensitive compounds used in this study. Their absorption spectra are shown in Figure 1b in the manuscript. The Ru complex can be cleaved by blue light. The o-nitrobenzyl derivative can be cleaved by UV light. Photochromism of azobenzene, spiropyran derivative, and diarylethene derivative from their stable states to metastable states can be induced by UV light.

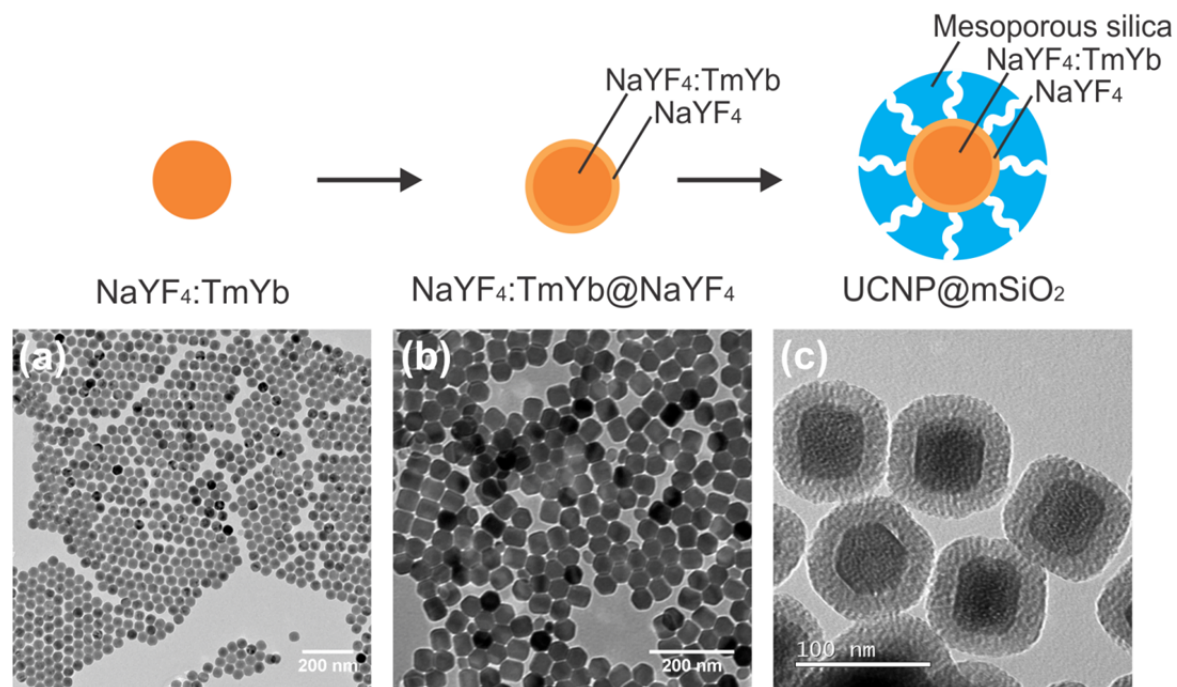


Figure S2. Synthetic procedure and TEM images of UCNPs: (a) NaYF₄:TmYb, (b) NaYF₄:TmYb@NaYF₄, (c) UCNP@mSiO₂. The average diameters for NaYF₄:TmYb, NaYF₄:TmYb@NaYF₄, and UCNP@mSiO₂ nanoparticles are 43, 50, and 92 nm, respectively. The average silica shell thickness for UCNP@mSiO₂ nanoparticles is 21 nm.

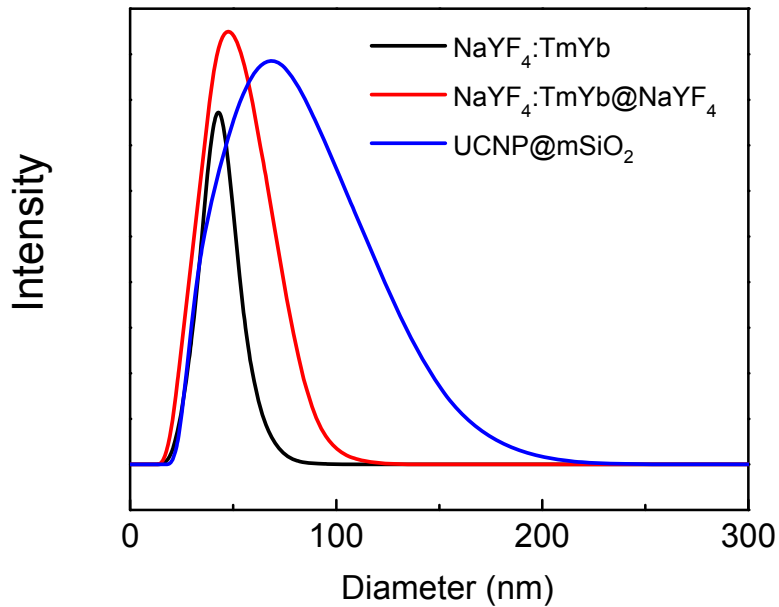


Figure S3. Size distributions of NaYF₄: TmYb (black line), NaYF₄:TmYb@NaYF₄ (red line), and UCNP@mSiO₂ (blue line) nanoparticles determined by dynamic light scattering (DLS). The average diameters for NaYF₄:TmYb, NaYF₄:TmYb@NaYF₄, and UCNP@mSiO₂ nanoparticles are 43, 48, and 89 nm, respectively.

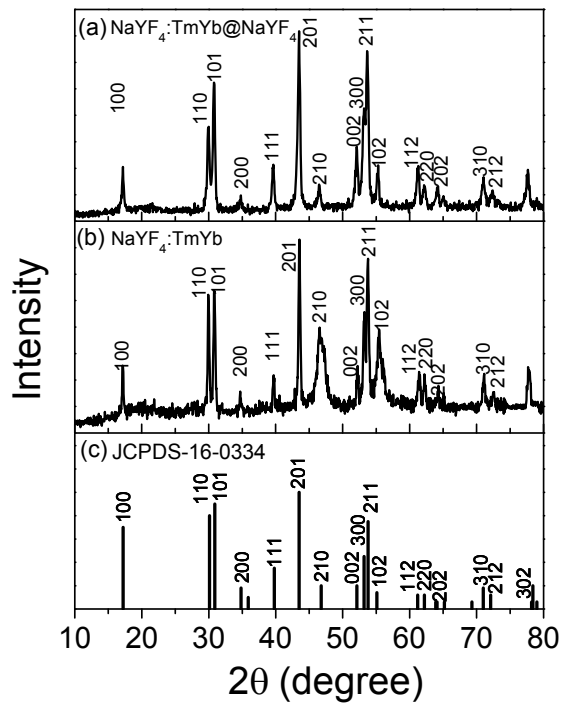


Figure S4. Powder X-ray diffraction (XRD) patterns for $\text{NaYF}_4:\text{TmYb}@NaYF_4$ (a) and $\text{NaYF}_4:\text{TmYb}$ nanoparticles (b). (c) JCPDS standard card No.16-0334 for hexagonal NaYF_4 crystal.

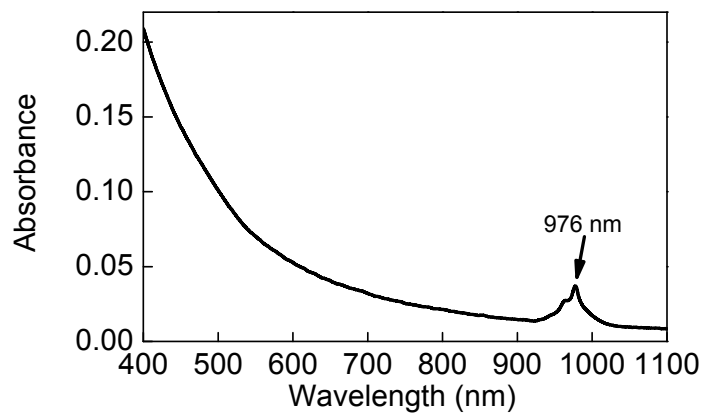


Figure S5. UV/Vis/NIR absorption spectrum of NaYF₄:TmYb@NaYF₄ UCNPs in cyclohexane. The absorption maximum is at 976 nm.

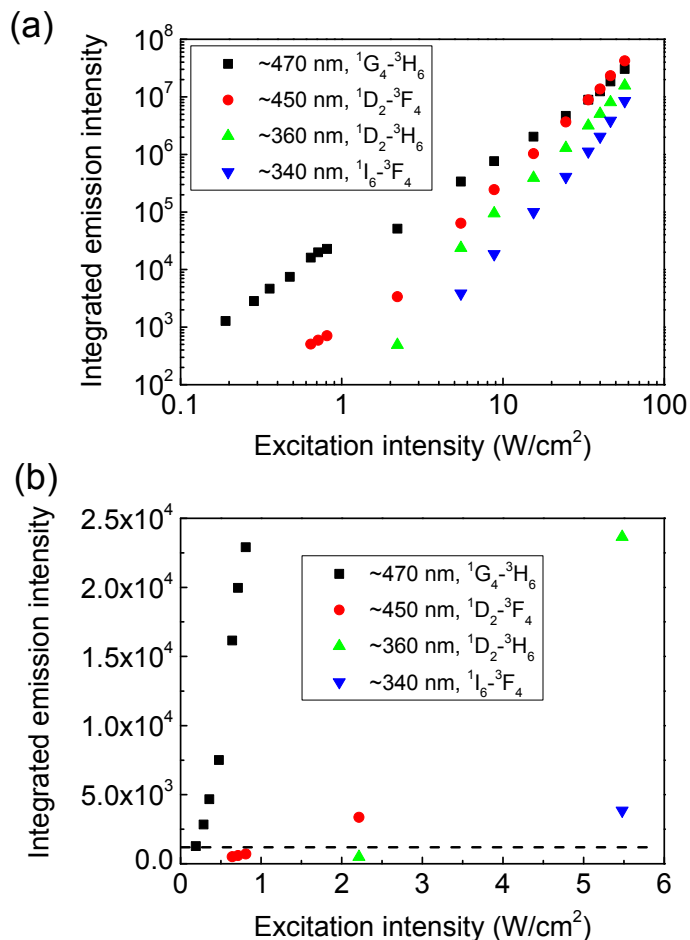


Figure S6. Emission intensity of NaYF₄:TmYb@NaYF₄ UCNPs upon 974 nm laser excitation with different excitation intensities: (a) Double logarithmic plot of integrated upconversion luminescence versus excitation intensity. (b) Plot of integrated upconversion luminescence versus excitation intensity at low-intensity region. The dashed line in (b) shows that the intensity of upconversion luminescence at ~470 nm under the excitation intensity 0.19 W/cm² is even higher than that at ~360 nm under the excitation intensity 2.2 W/cm². This result indicates that UCNP-assisted photochemistry for blue-light-sensitive compounds might be more efficient under 0.19 W/cm² than that for UV-sensitive compounds under 2.2 W/cm².

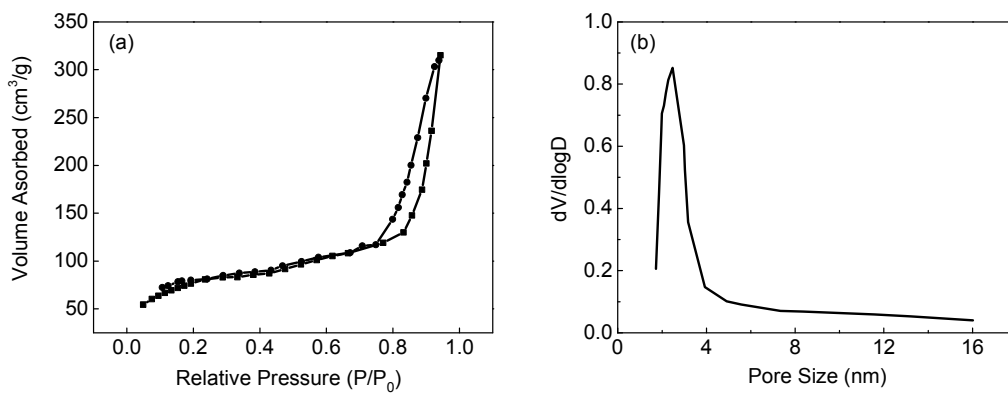


Figure S7. N₂ adsorption-desorption isotherm (a) and pore size distribution (b) of UCNP@mSiO₂. The average BET surface area and the average pore size determined by this measurement are ~316 m²/g and ~2.6 nm, respectively.

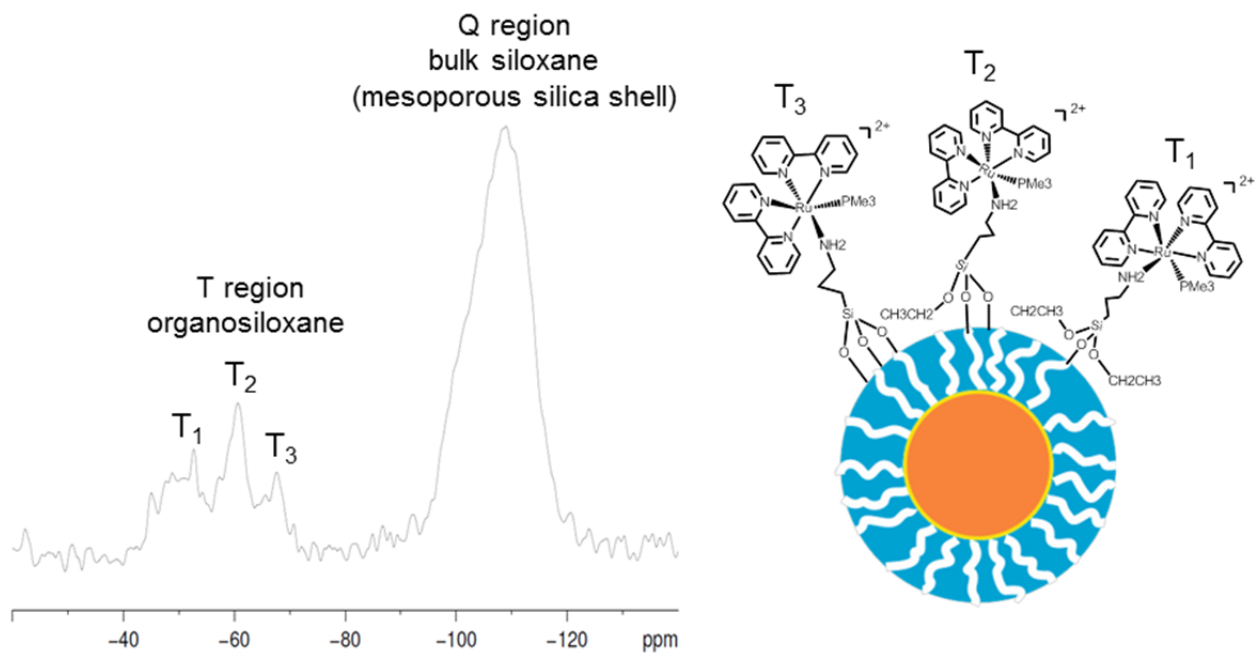


Figure S8. ^{29}Si MAS solid-state NMR spectrum and schematic illustration of UCNP@mSiO₂-Ru nanoparticles. The spectrum shows two regions at around -60 and -110 ppm, which are corresponding to the organosiloxane (T region) and bulk siloxane (Q region), respectively.^[8] The three bands T1, T2, T3 indicate that siloxane groups in the Ru complex may hydrolyze in three different ways (see schematic model).^[8] This result shows that Ru1 is grafted on UCNP@mSiO₂ nanoparticles.

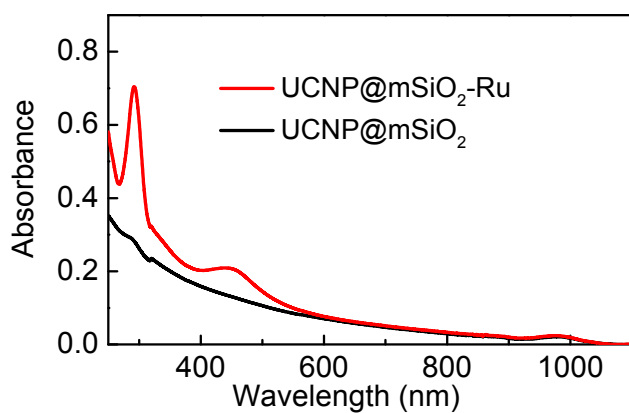


Figure S9. UV/Vis/NIR absorption spectra of UCNP@mSiO₂ and UCNP@mSiO₂-Ru nanoparticles. The band at ~976 nm belongs to the UCNPs. The band at ~450 nm is the metal-to-ligand charge transfer (MLCT) band of the Ru complex. The band at ~290 nm is assigned to π - π^* transition of the bipyridine ligand in the Ru complex.

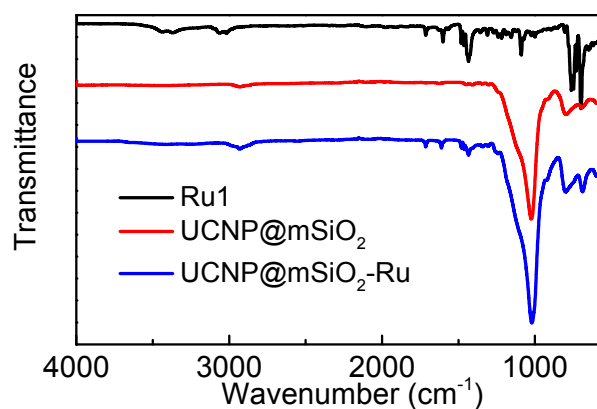


Figure S10. FTIR spectra of the Ru complex (Ru1), UCNP@mSiO₂ and UCNP@mSiO₂-Ru. In the spectrum of Ru1, the band at 1601 cm⁻¹ and the bands in the region 1400-1490 cm⁻¹ are assigned to stretching modes of the bipyridine rings.^[9] The bands in the region 730-790 cm⁻¹ are assigned to C-H out-of-plane bending.^[10] In the spectrum of UCNP@mSiO₂, the broad band in the region 1000-1100 cm⁻¹ is assigned to Si-O-Si asymmetric stretching.^[11] The band at ~795 cm⁻¹ is assigned to the Si-O-Si symmetric stretching.^[11] Characteristic bands of both Ru1 and UCNP@mSiO₂ appear in the spectrum of UCNP@mSiO₂-Ru.

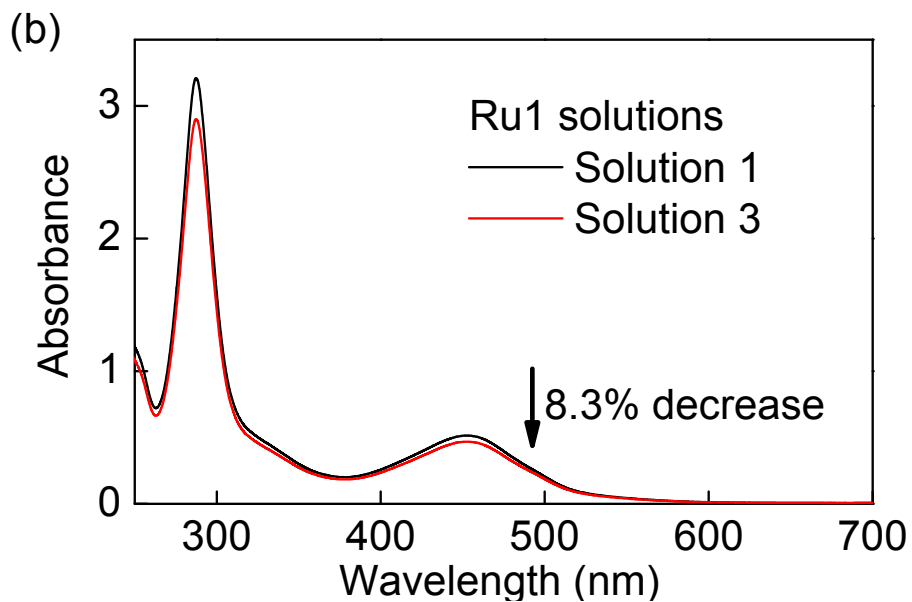
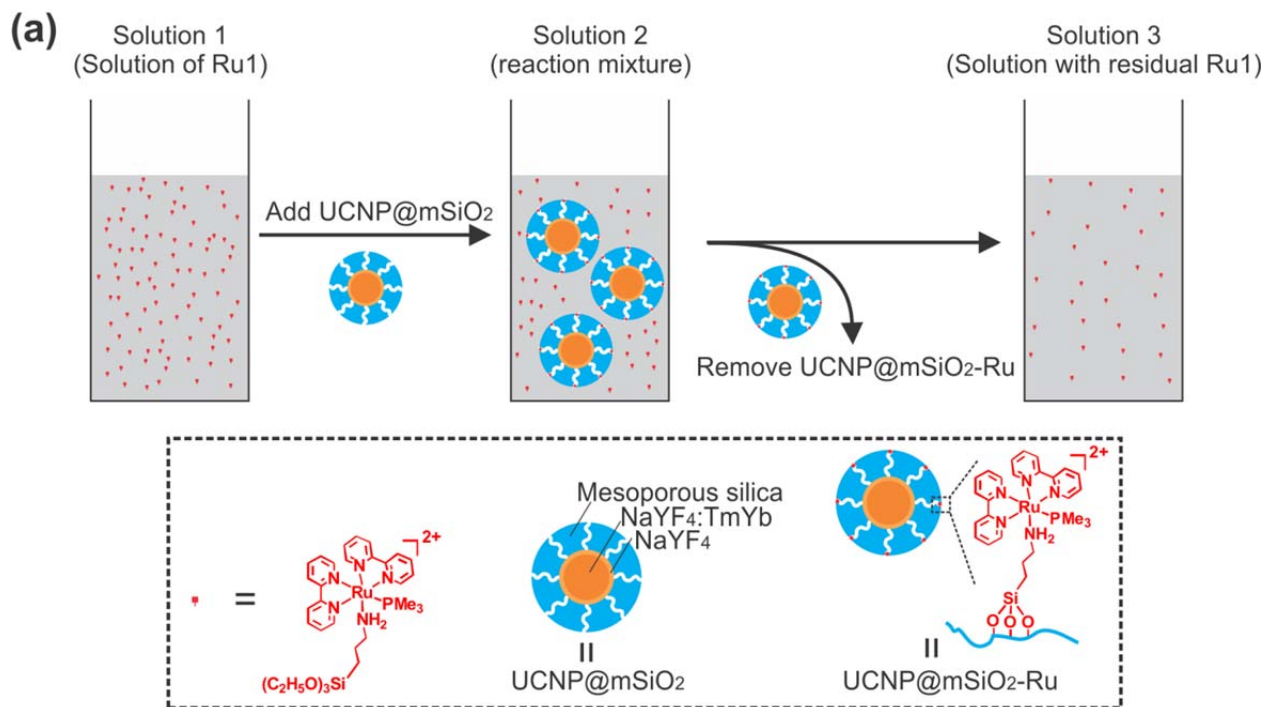


Figure S11. Procedure to measure the content of the Ru complexes grafted on UCNP@mSiO₂: (a) Schematic illustration of the procedure. (b) UV/Vis absorption spectra of Solution 1 and Solution 3. We calculated the amount of Ru complex grafted on UCNP@mSiO₂ by the absorption spectra. There was $\sim 7.6 \mu\text{g}$ Ru1 grafted on 1 mg UCNP@mSiO₂ nanoparticles.

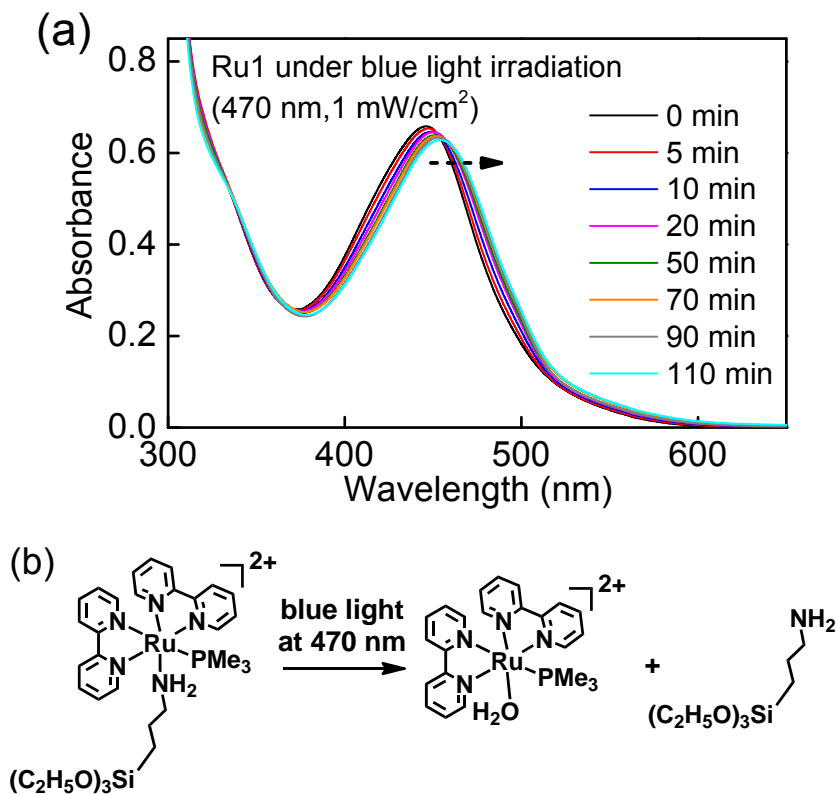


Figure S12. (a) UV/Vis absorption spectra of Ru1 before (0 min) and after irradiation with 470 nm light (1 mW/cm²) for 5, 10, 20, 50, 70, 90, and 110 min. The metal-to-ligand charge transfer band shifted to longer wavelength, which indicates the cleavage of the Ru complex. This spectral change is the same as those recorded when Ru1 or similar Ru complexes are exposed to blue light to trigger photocleavage.^[4, 12] (b) The photoreaction of Ru1 induced by blue light.

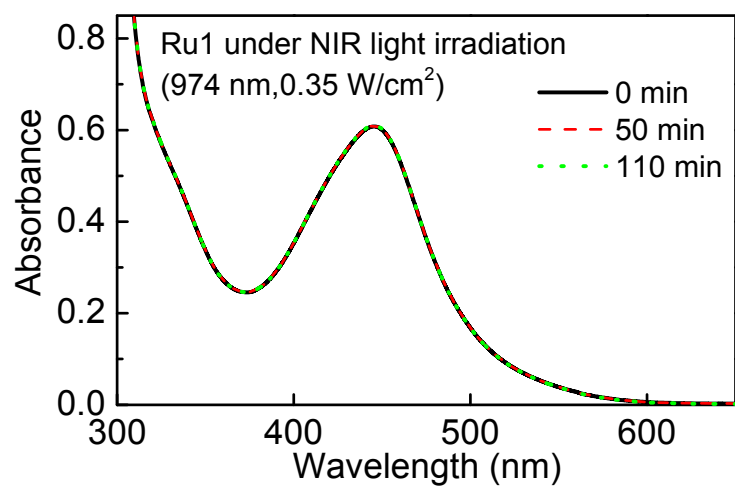


Figure S13. UV/Vis absorption spectra of Ru1 before (0 min) and after irradiation with 974 nm light (0.35 W/cm^2) for 50 and 110 min. This result indicates that Ru1 in the absence of UCNPs cannot be cleaved by 974 nm light directly.

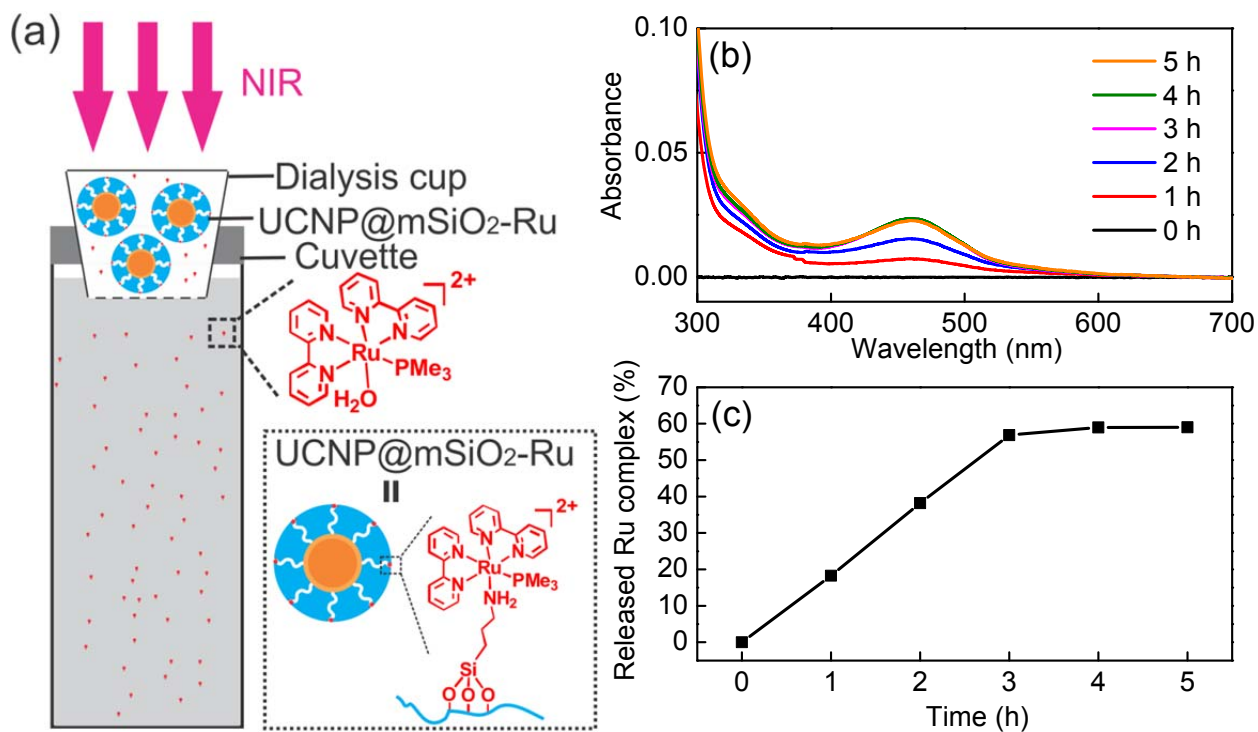


Figure S14. Determination of the amount of the released Ru complex by “mini dialysis”: (a) schematic model of the experimental setup. (b) UV/Vis absorption spectra of the released Ru complexes in the cuvette. (c) Amount of released Ru complexes calculated by the spectra in (b).

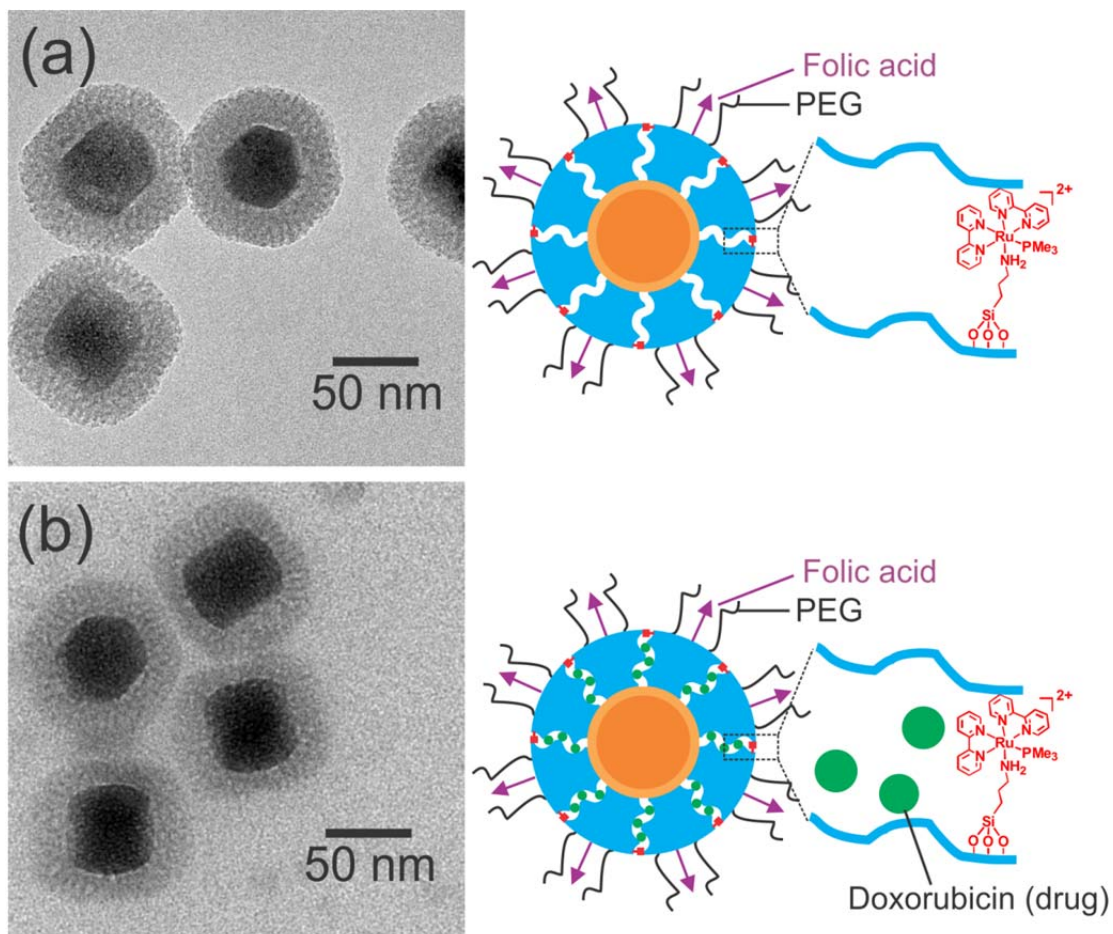


Figure S15. TEM images and schematic models of PEG- and FA-modified UCNP@mSiO₂-Ru (a) and PEG- and FA-modified DOX-UCNP@mSiO₂-Ru (b). The morphology of the nanoparticles retained after surface modification.

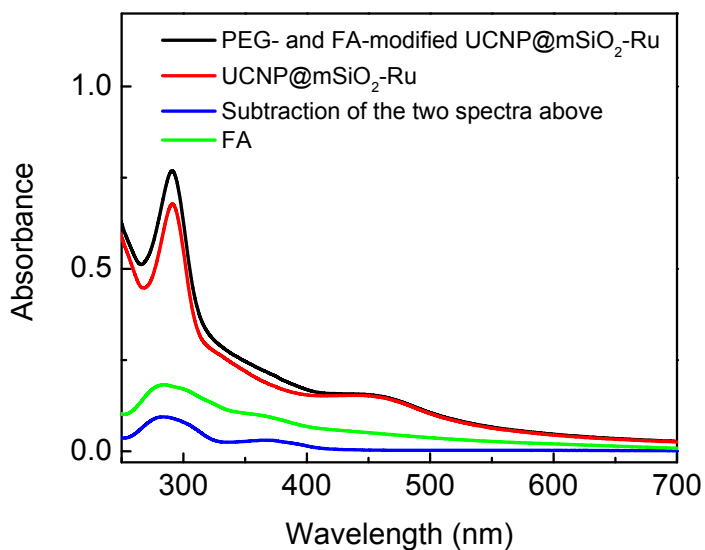


Figure S16. UV/Vis absorption spectra of folic acid (FA), UCNP@mSiO₂-Ru nanoparticles and PEG- and FA-modified UCNP@mSiO₂-Ru nanoparticles. We compared the spectrum of pure FA and the subtraction spectrum. The bands of the two spectra are identical, which indicates FA is on the surface of the nanoparticles. Additionally, we calculated the amount of FA on the surface of nanoparticles by the UV/Vis absorption spectra. There is ~1.25 μg FA on 1 mg nanoparticles.

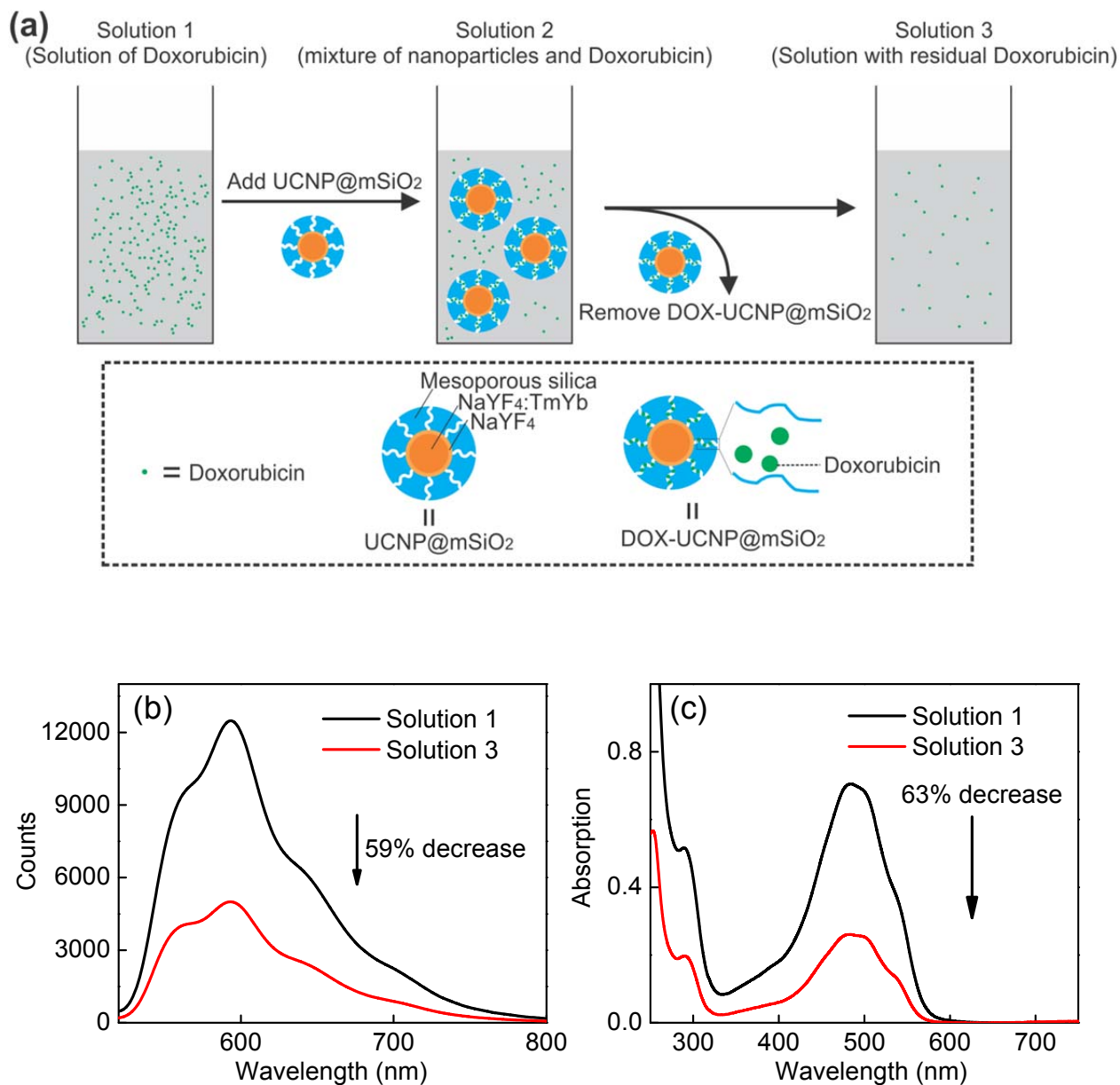


Figure S17. Procedure to determine the loading efficiency of doxorubicin in UCNP@mSiO₂: (a) Schematic illustration of the procedure. (b) Fluorescence spectra (λ_{ex} = 480 nm) and (c) UV/Vis absorption spectra of Solution 1 and Solution 3. The drug loading efficiency measured by fluorescence spectroscopy and UV/Vis absorption spectroscopy is 2.36% and 2.52% (23.6 and 25.2 μg doxorubicin in 1 mg nanoparticles), respectively.

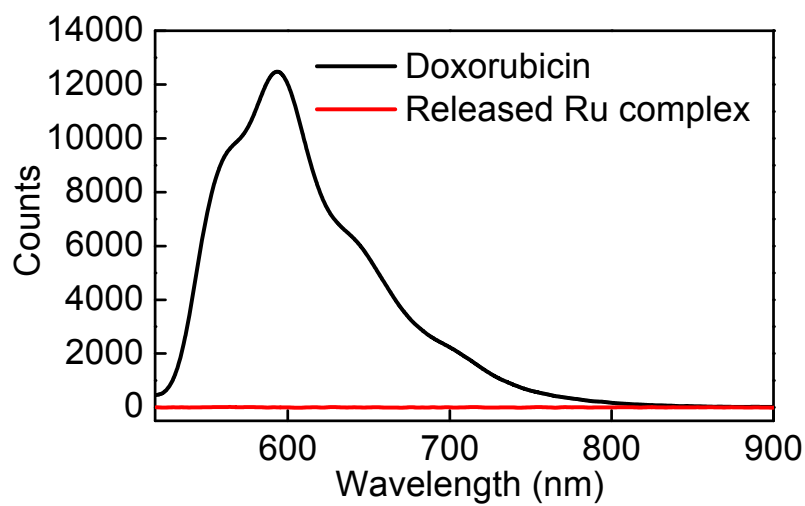


Figure S18. Fluorescence spectra ($\lambda_{\text{ex}} = 480 \text{ nm}$) of doxorubicin ($\sim 6.9 \times 10^{-5} \text{ mol/L}$ in water) and the released Ru complex ($\sim 6.9 \times 10^{-5} \text{ mol/L}$ in water). The released Ru complex is non-fluorescent.

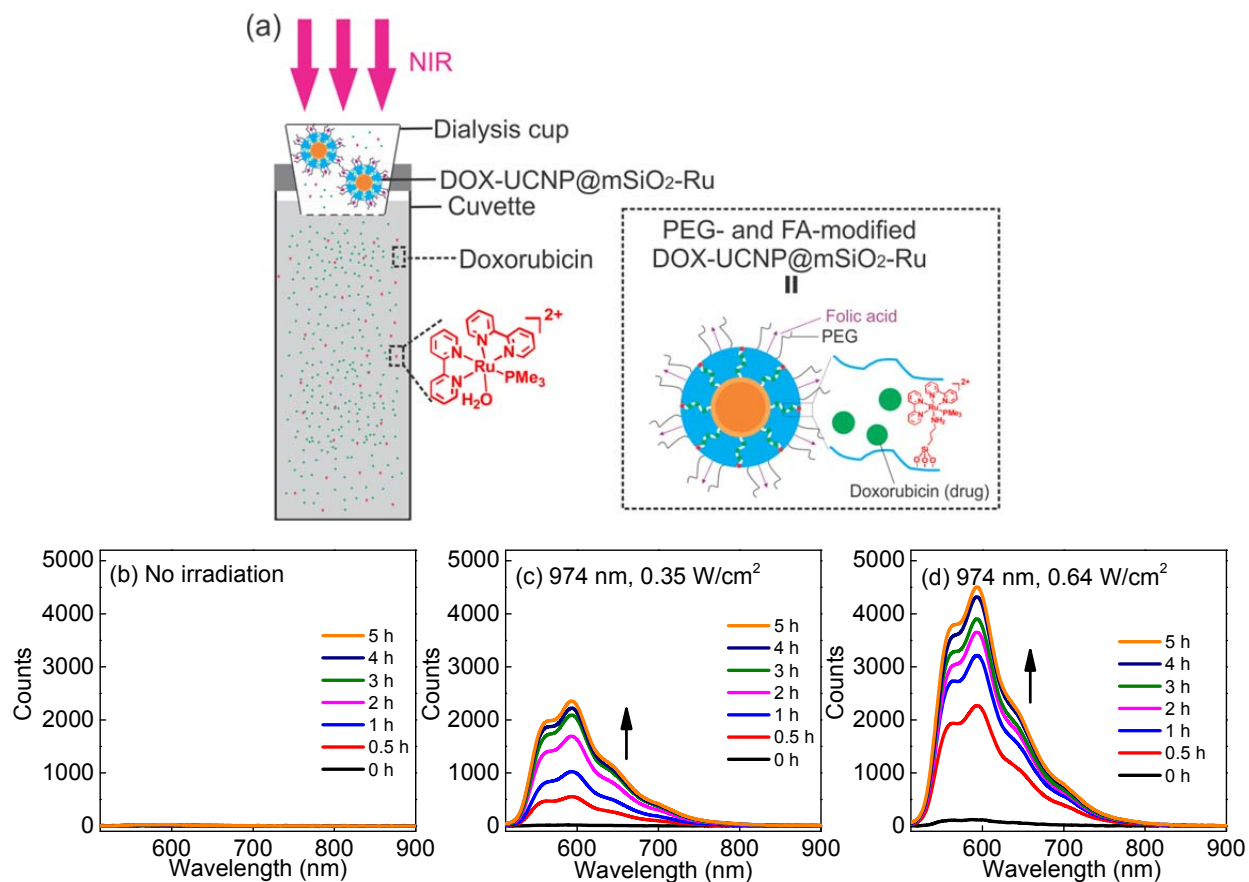


Figure S19. Determination of the amount of released doxorubicin by “mini dialysis”: (a) schematic model of the experimental setup. (b)-(d) Fluorescence spectra ($\lambda_{\text{ex}} = 480 \text{ nm}$) of released doxorubicin in the cuvette at different irradiation conditions: (b) No irradiation, (c) NIR irradiation (974 nm , 0.35 W/cm^2), and (d) NIR irradiation (974 nm , 0.64 W/cm^2). The percentage of released doxorubicin is shown in Figure 3c in the manuscript.

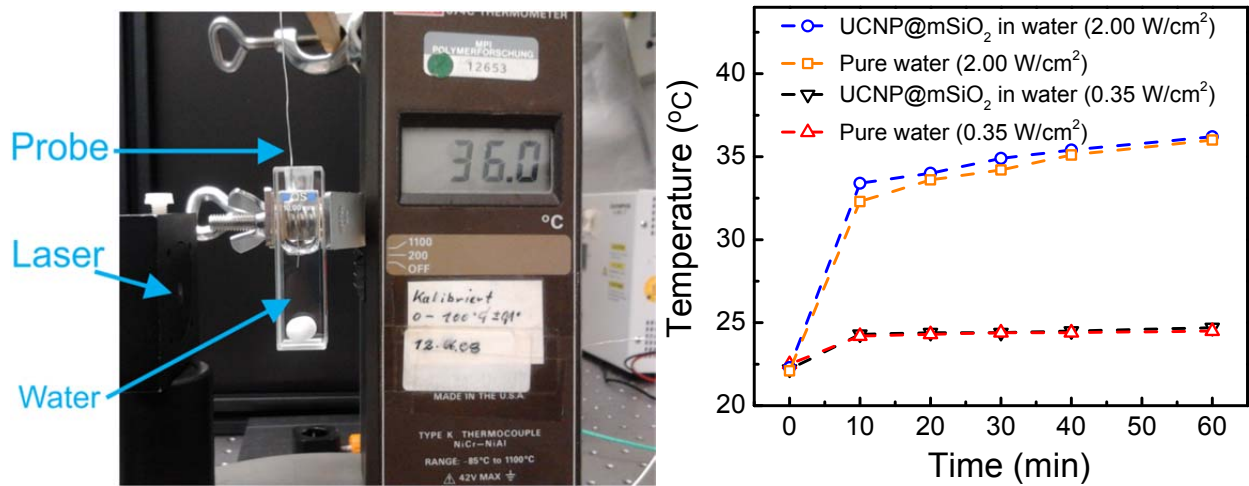
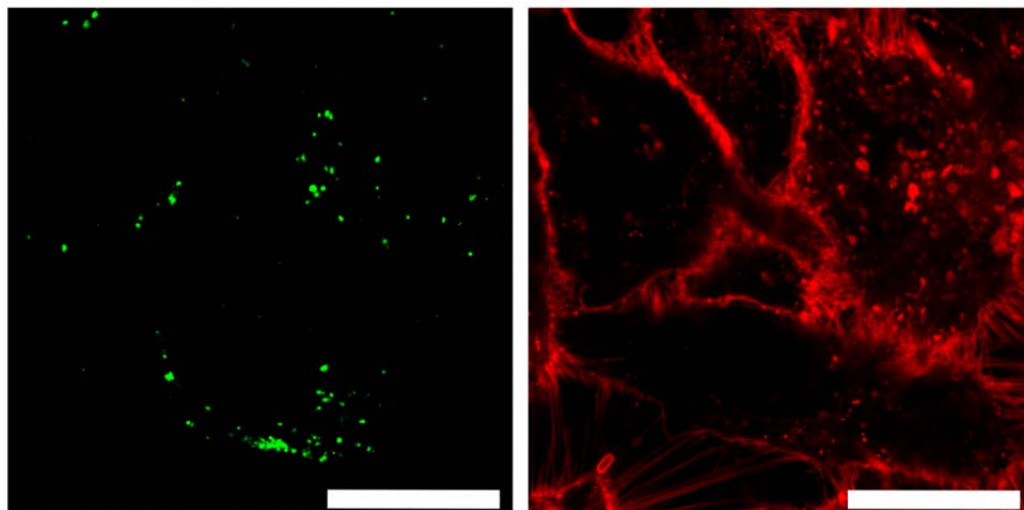


Figure S20. Temperature increase of water and dispersion of UCNP@mSiO₂ nanoparticles (1 mg/mL in water) under continuous irradiation of 974 nm light under 0.35 W/cm² and 2.00 W/cm².

(a) UCNP@mSiO₂-Ru-FITC (b) Cell membrane



(c) Nucleus

(d) Merged image of (a), (b) and (c)

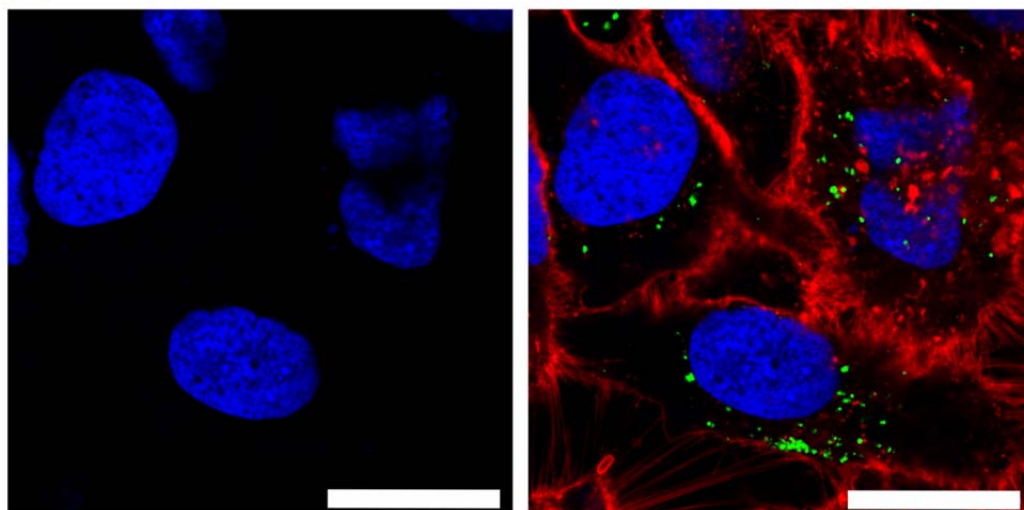


Figure S21: Confocal laser scanning microscopy image: fluorescence-labeled UCNP@mSiO₂-Ru nanoparticles are taken up by HeLa cells. Single channel pictures of (a) UCNP@mSiO₂-Ru-FITC (green), (b) the cell membrane (red, CellMaskOrange), and (c) nucleus (blue, Draq5). (d) Merged image of (a), (b), and (c). The scale bars are 25 μ m. Three dimensional images viewed from with yz and xz plains are shown in Figure 4a in the manuscript.

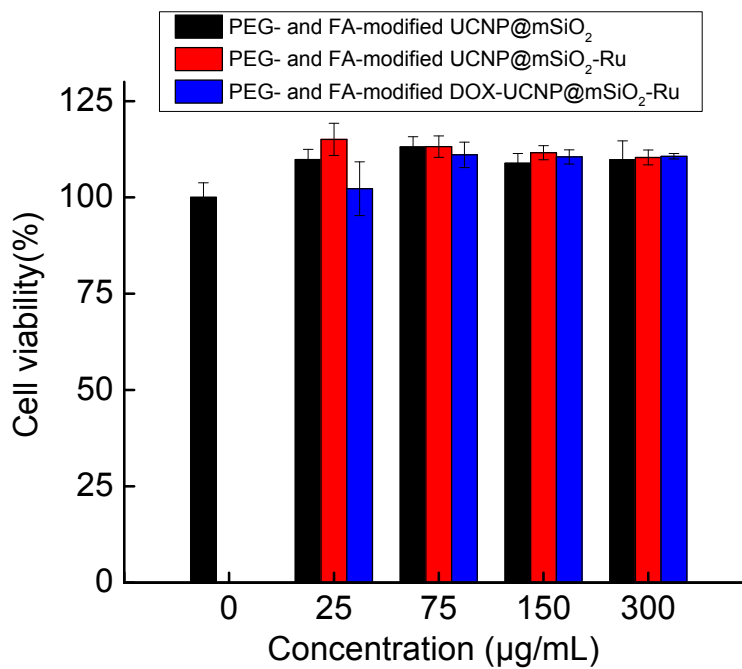


Figure S22. Viability of HeLa cells incubated for 24 h in the presence of different nanoparticles with different concentrations.

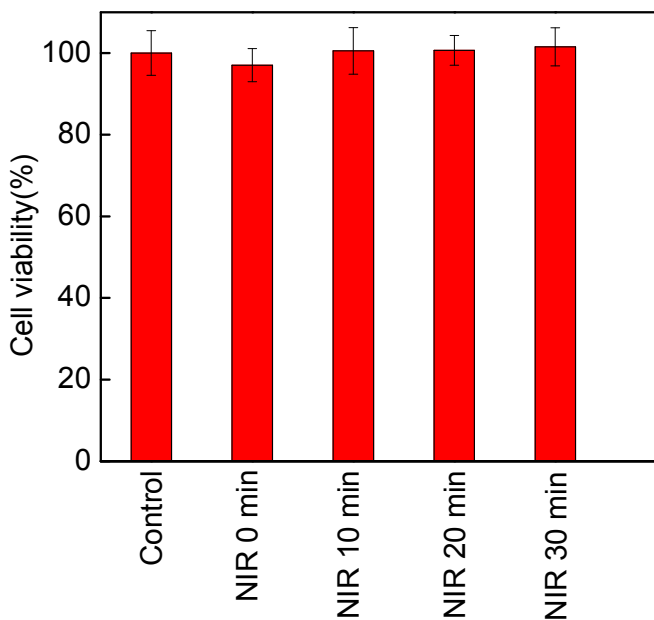


Figure S23. Effects of light exposure (974 nm, 0.35 W/cm²) on the viability of HeLa cells in the absence of nanoparticles for different time. Control: Cells in the absence of nanoparticles under room conditions.

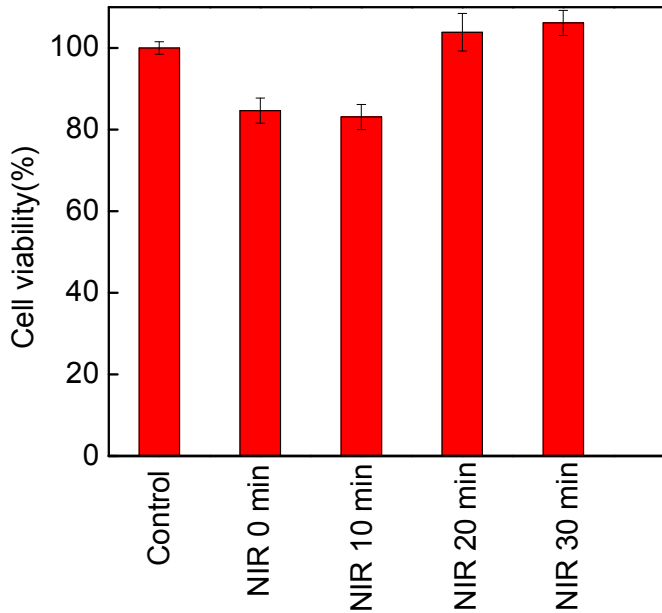


Figure S24. Effects of light exposure (974 nm, 0.35 W/cm²) on the viability of HeLa cells in the presence of PEG- and FA-modified UCNPs@*m*SiO₂ nanoparticles for different time. Control: Cells in the absence of nanoparticles under room conditions.

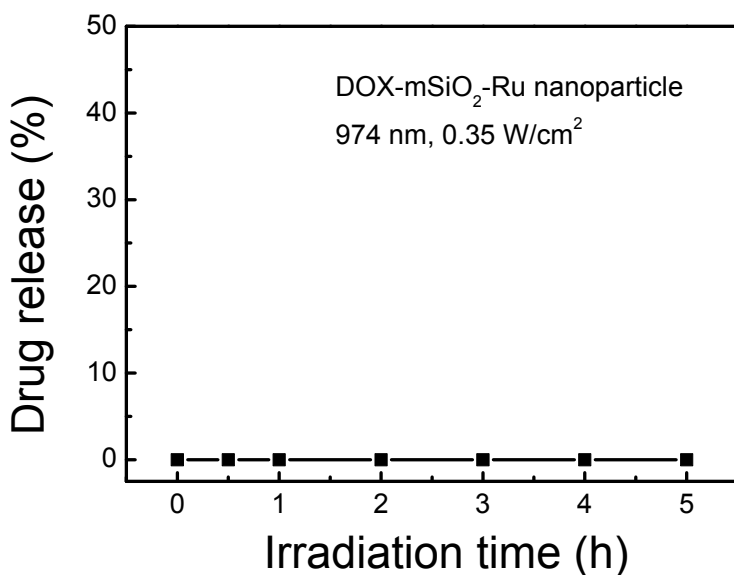


Figure S25. Doxorubicin release profile for PEG- and FA- functionalized DOX-mSiO₂-Ru nanoparticles upon 974 nm light exposure (0.35 W/cm²). In this control experiment, we used MCM-41 type mesoporous silica nanoparticles (Sigma Aldrich, CAS No. 7631-86-9, pore size 2.1-2.7 nm) instead of UCNP@mSiO₂ nanoparticles to fabricate drug carriers. There is no upconversion core in DOX-mSiO₂-Ru nanoparticles. This control experiment confirms that NIR light could not directly induce drug release using nanoparticles without upconversion cores.

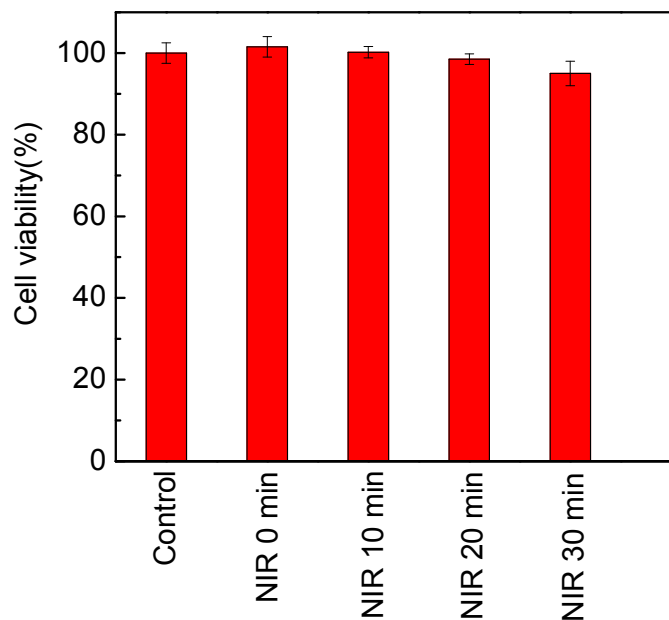
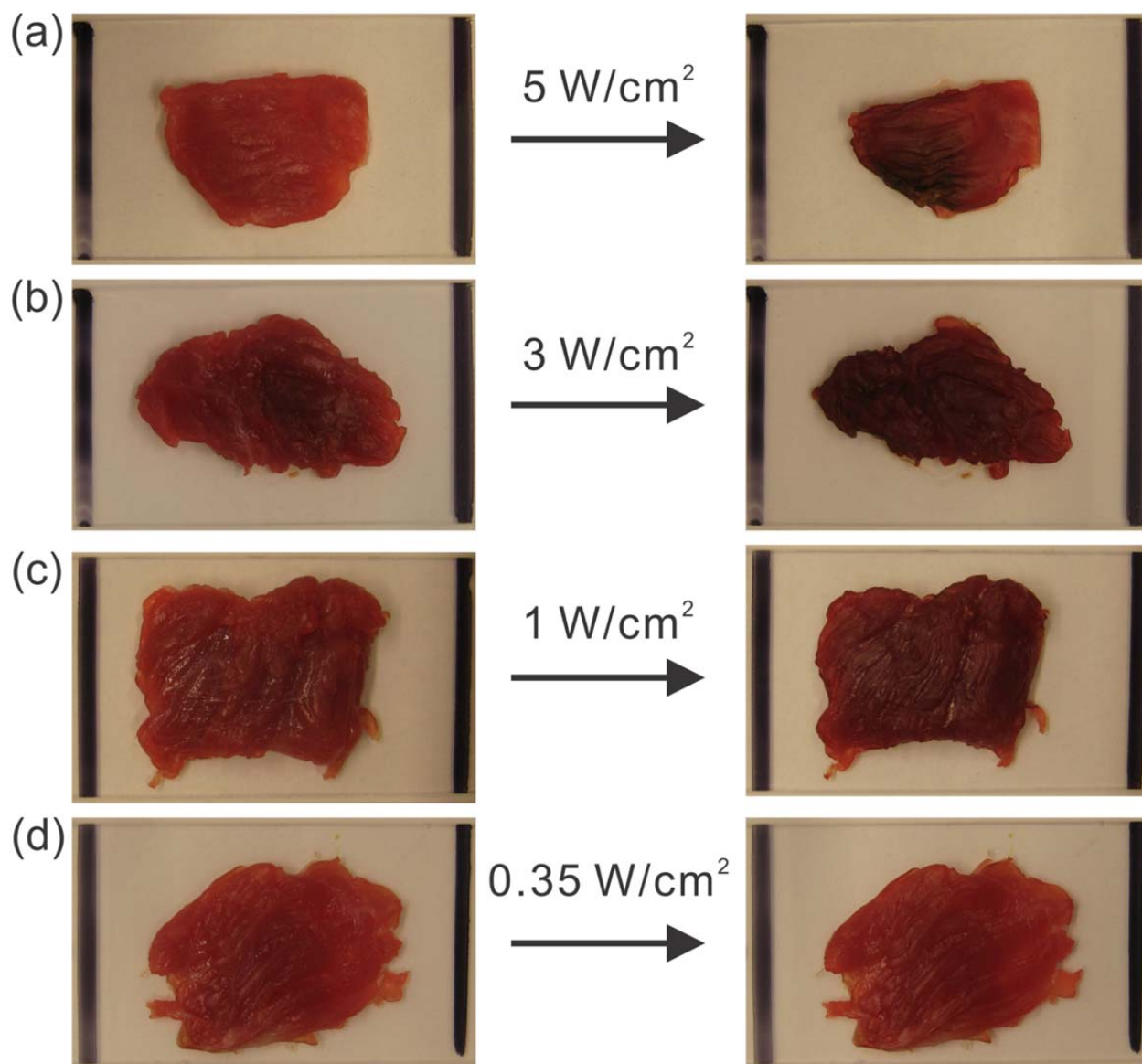


Figure S26. Effects of light exposure (974 nm, 0.35 W/cm²) on the viability of HeLa cells in the presence of PEG- and FA- functionalized DOX-mSiO₂-Ru nanoparticles for different time. Control: Cells in the absence of nanoparticles under room conditions. In this experiment, we used MCM-41 type mesoporous silica nanoparticles (Sigma Aldrich, CAS No. 7631-86-9, pore size 2.1-2.7 nm) instead of UCNP@mSiO₂ nanoparticles to fabricate drug carriers. There is no upconversion core in DOX-mSiO₂-Ru nanoparticles. Without upconversion cores in the nanoparticles, NIR light could not inhibit the growth of cancer cells.



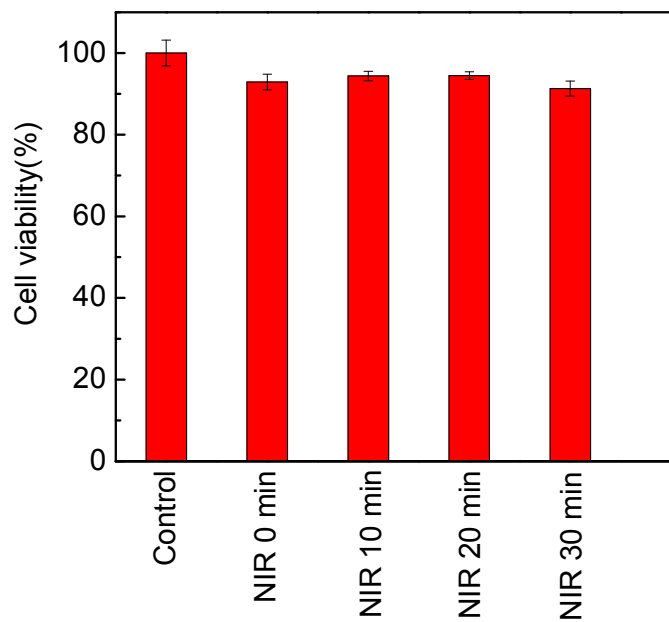


Figure S28. Effects of light exposure (974 nm, 0.64 W/cm²) on the viability of HeLa cells in the absence of nanoparticles for different time. Control: Cells in the absence of nanoparticles under room conditions.

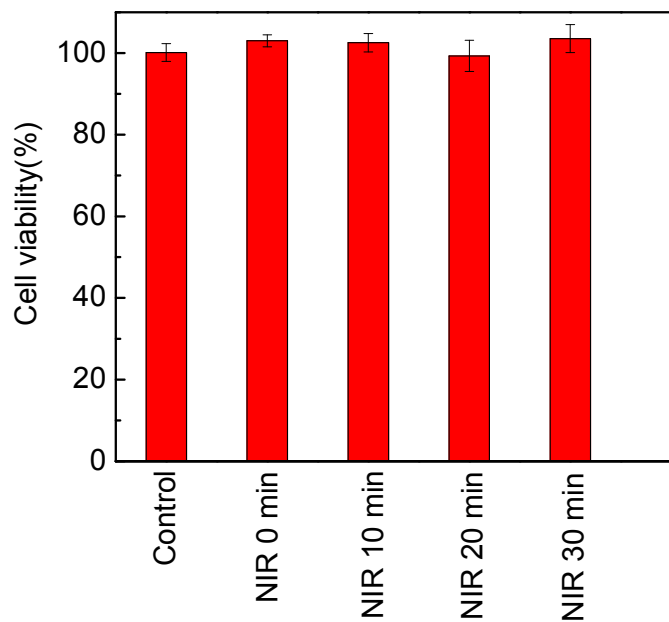


Figure 29. Effects of light exposure (974 nm, 0.64 W/cm²) on the viability of HeLa cells in the presence of PEG- and FA-modified UCNP@mSiO₂-Ru nanoparticles for different time. Control: Cells in the absence of nanoparticles under room conditions.

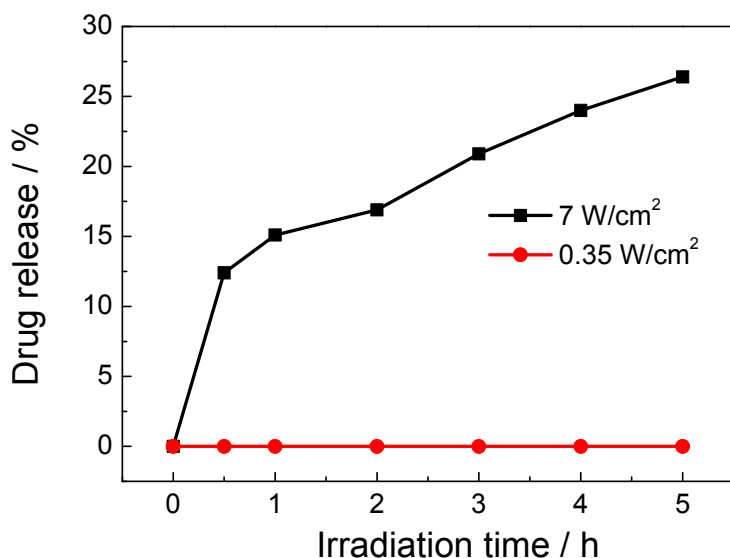


Figure S30. Doxorubicin release profile for DOX-UCNP@mSiO₂-azo nanoparticles. To make an experimental comparison with other systems, we synthesized DOX-UCNP@mSiO₂-azo nanoparticles that were reported in a recent paper.^[13] In this system, upconverted UV light induced photoisomerization of azobenzene and subsequent drug release.^[13] At low excitation intensity (0.35 W/cm²), no release could be detected. At high excitation intensity (7 W/cm²), approximately 26 % of doxorubicin was released after 974 nm light irradiation for 5 hours. This result strongly supports our hypothesis that low intensity 974 nm light cannot trigger photoreaction of UV sensitive compounds such as azobenzene. Compared with the DOX-UCNP@mSiO₂-azo nanoparticles, the UCNP@mSiO₂-Ru nanoparticles reported in this paper need much lower light intensity (0.35 W/cm²) to trigger drug release. The low-intensity NIR light can minimize photodamages to tissue (Figure S27).

Table S1. Summary of reported UCNP-assisted photochemistry

UCNP	photosensitive chromophore	λ_{\max} (nm) ^h	intensity (W/cm ²)	photoreaction
NaYF ₄ :TmYb@NaYF ₄	o-nitrobenzyl	350	2.8 [14], 5.6 [15], 255 [16], 16 [17] ^a , Unknown [7b, 18] ^b	cleavage
NaYF ₄ :TmYb@CaF ₂	o-nitrobenzyl	350	2.6 [19]	cleavage
NaYF ₄ :TmYb@NaYF ₄	azobenzene	330	2.4 [13]	isomerization
NaYF ₄ :TmYb	azotolane	385	15 [20]	isomerization
LiYF ₄ :TmYb	spiropyrane	333	Unknown [21] ^b	isomerization
Various UCNPs ^c	Dithienylethene	300-350 ^d , 520-620 ^e	150-500 [2, 22] ^f , 15 [2] ^g	isomerization
NaYF ₄ :TmYb	dialkoxybenzoin	290	550 [23]	photolysis
NaYF ₄ :TmYb@NaGdF ₄ :Yb	platinum complex	289	2.5 [24]	activation
NaYF ₄ :TmYb@NaYF ₄	Ru1	453	0.35 [this work]	cleavage

^aCalculated from the reported power and beam diameter; ^bThe authors reported the laser power only and did not report the power density nor the beam diameter; ^cNaYF₄:ErYb, NaYF₄:TmYb, and core-shell-shell nanoparticles (core and inner shell = NaYF₄:ErYb or NaYF₄:TmYb, outer shell = NaYF₄); ^dring-open isomer; ^ering-closed isomer; ^fring-closing reaction; ^gring-opening reaction; ^habsorption maximum of photosensitive chromophores.

References

- [1] V. San Miguel, C. G. Bochet, A. del Campo, *J. Am. Chem. Soc.* **2011**, *133*, 5380-5388.
- [2] J. C. Boyer, C. J. Carling, B. D. Gates, N. R. Branda, *J. Am. Chem. Soc.* **2010**, *132*, 15766-15772.
- [3] a) T. Kim, E. Momin, J. Choi, K. Yuan, H. Zaidi, J. Kim, M. Park, N. Lee, M. T. McMahon, A. Quinones-Hinojosa, J. W. M. Bulte, T. Hyeon, A. A. Gilad, *J. Am. Chem. Soc.* **2011**, *133*, 2955-2961; b) J. Kim, H. S. Kim, N. Lee, T. Kim, H. Kim, T. Yu, I. C. Song, W. K. Moon, T. Hyeon, *Angew. Chem. Int. Ed.* **2008**, *47*, 8438-8441.
- [4] V. S. Miguel, M. Alvarez, O. Filevich, R. Etchenique, A. del Campo, *Langmuir* **2012**, *28*, 1217-1221.
- [5] C. Li, D. Yang, P. Ma, Y. Chen, Y. Wu, Z. Hou, Y. Dai, J. Zhao, C. Sui, J. Lin, *Small* **2013**, *9*, 4150-4159.
- [6] Y. K. Peng, C. W. Lai, C. L. Liu, H. C. Chen, Y. H. Hsiao, W. L. Liu, K. C. Tang, Y. Chi, J. K. Hsiao, K. E. Lim, H. E. Liao, J. J. Shyue, P. T. Chou, *ACS Nano* **2011**, *5*, 4177-4187.
- [7] a) N. Singh, A. Karambelkar, L. Gu, K. Lin, J. S. Miller, C. S. Chen, M. J. Sailor, S. N. Bhatia, *J. Am. Chem. Soc.* **2011**, *133*, 19582-19585; b) B. Yan, J. C. Boyer, N. R. Branda, Y. Zhao, *J. Am. Chem. Soc.* **2011**, *133*, 19714-19717.
- [8] a) S. L. Burkett, S. D. Sims, S. Mann, *Chem. Commun.* **1996**, 1367-1368; b) E. Lindner, R. Schreiber, M. Kemmler, T. Schneller, H. A. Mayer, *Chem. Mater.* **1995**, *7*, 951-960.
- [9] a) K. M. Omberg, J. R. Schoonover, J. A. Treadway, R. M. Leasure, R. B. Dyer, T. J. Meyer, *J. Am. Chem. Soc.* **1997**, *119*, 7013-7018; b) A. Y. Kuposov, T. Cardolaccia, V. Albert, E. Badaeva, S. Kilina, T. J. Meyer, S. Tretiak, M. Sykora, *Langmuir* **2011**, *27*, 8377-8383.
- [10] P. Li, W. Su, J. Cui, L. Huo, N. Guo, Y. Huang, *International Proceedings of Computer Science & Information Tech.* **2012**, *51*, 82-88.
- [11] J. Y. Bae, S. H. Choi, B. S. Bae, *Bulletin of the Korean Chemical Society* **2006**, *27*, 1562-1566.
- [12] a) L. Zayat, M. G. Noval, J. Campi, C. I. Calero, D. J. Calvo, R. Etchenique, *ChemBioChem* **2007**, *8*, 2035-2038; b) R. E. Goldbach, I. Rodriguez-Garcia, J. H. van Lenthe, M. A. Siegler, S. Bonnet, *Chem.-Eur. J.* **2011**, *17*, 9924-9929.
- [13] J. Liu, W. Bu, L. Pan, J. Shi, *Angew. Chem. Int. Ed.* **2013**, *52*, 4375-4379.
- [14] M. K. G. Jayakumar, N. M. Idris, Y. Zhang, *Proc. Natl. Acad. Sci. USA* **2012**, *109*, 8483-8488.
- [15] Y. Yang, B. Velmurugan, X. Liu, B. Xing, *Small* **2013**, *9*, 2937-2944.
- [16] Y. M. Yang, Q. Shao, R. R. Deng, C. Wang, X. Teng, K. Cheng, Z. Cheng, L. Huang, Z. Liu, X. G. Liu, B. G. Xing, *Angew. Chem. Int. Ed.* **2012**, *51*, 3125-3129.
- [17] M. L. Viger, M. Grossman, N. Fomina, A. Almutairi, *Adv. Mater.* **2013**, *25*, 3733-3738.
- [18] B. Yan, J. C. Boyer, D. Habault, N. R. Branda, Y. Zhao, *J. Am. Chem. Soc.* **2012**, *134*, 16558-16561.
- [19] J. Shen, G. Chen, T. Y. Ohulchansky, S. J. Kesseli, S. Buchholz, Z. Li, P. N. Prasad, G. Han, *Small* **2013**, *9*, 3213-3217.
- [20] W. Wu, L. M. Yao, T. S. Yang, R. Y. Yin, F. Y. Li, Y. L. Yu, *J. Am. Chem. Soc.* **2011**, *133*, 15810-15813.
- [21] B. F. Zhang, M. Frigoli, F. Angiuli, F. Vetrone, J. A. Capobianco, *Chem. Commun.* **2012**, *48*, 7244-7246.
- [22] C. J. Carling, J. C. Boyer, N. R. Branda, *J. Am. Chem. Soc.* **2009**, *131*, 10838-10839.
- [23] C. J. Carling, F. Nourmohammadian, J. C. Boyer, N. R. Branda, *Angew. Chem. Int. Edit.* **2010**, *49*, 3782-3785.
- [24] Y. Dai, H. Xiao, J. Liu, Q. Yuan, P. Ma, D. Yang, C. Li, Z. Cheng, Z. Hou, P. Yang, J. Lin, *J. Am. Chem. Soc.* **2013**, *135*, 18920-18929.